Growth and characterization of zinc doped l-proline cadmium chloride monohydrate single crystals for non linear optical applications and UV sensors

S. VETRIVEL*, R. RAJASEKARAN, K. KANAGASABAPATHY[a], S. GOPINATH[b], SUMAN BHATTACHARYA[c], R. RAJASEKARAN

P.G.& Research Department of Physics, Government Arts College, Tiruvannamalai-606603, Tamil Nadu, India
[a]P.G.& Research Department of Physics, A. A. Government Arts College, Villupuram-605602 , Tamil Nadu, India
[b]Arunai Engineering College, Tiruvannamalai, Tamil Nadu-606603, India
[c]Department of Chemistry, Pondicherry University, Pondicherry-605 014, India

Single crystals of zinc doped L–proline cadmium chloride monohydrate (Zn:LPCCM) with size about 47×14×3.7 mm^3has been successfully grown from aqueous solution by slow evaporation method at room temperature. The single crystal X-ray diffraction analysis has been carried out to find the lattice parameters and powder X-Ray diffraction patterns has been recorded and indexed for the analysis of crystalline nature of grown material. The presence of functional group has been confirmed by FTIR analysis. The optical transmittance spectrum has been recorded in wavelength region 100 nm to 1000 nm. The thermal properties has been studied by TGA/DTA cures. The second harmonic generation (SHG) test has been carried out and it reveals the NLO property of the crystals. The mechanical properties have been studied by microhardness measurement. The photo conducting nature of the grown crystal has been estimated by using both dark current and photo current studies. The incorporation of the impurity (zinc chloride) entered into L-proline cadmium chloride monohydrate crystals [L-PCCM] has been confirmed by SEM-EDX analysis. The electrical properties have been studied by Impedance spectroscopic analysis.

(Received March 1, 2012; accepted June 6, 2012)

Keywords: Crystal growth, XRD, FTIR, UV-Visible-NIR, TGA/DTA, NLO, SHG

1. Introduction

The field of Non Linear Optics (NLO) has been attracting the materials scientists for the past few decades due to their importance in providing the key functions of device fabrication. The NLO materials play a vital role in science and technology because of its variety of applications like frequency shifting, optical modulation, and optical memory for the emerging technologies in areas like telecommunications, signals processing, and optical interconnections [1-3]. Inorganic NLO materials are possessing high melting point, high mechanical strength, and high degree of chemical inertness but poor optical nonlinearity [4]. Organic compounds possess a high degree of delocalization due to their weak Van der Waal's and hydrogen bonding. Hence organic compounds are optically more nonlinear than inorganic materials [5]. Some of the advantages of organic materials include flexibility in the methods of synthesis, scope for altering the properties by functional substitution, inherently high nonlinearity, high damage resistance [6], but it is very difficult to grow large in size. To remove this discrepancy, scientists adopted different alternate strategies. The obvious one was to develop hybrid organic-inorganic materials with some tradeoff in their respective advantages. This new class of materials are known as semi organics [7]. One approach, to high efficient optical quality organic-based NLO materials, in this class is to form compounds in which a polarizable organic molecule is stochiometrically bonded to an inorganic host. Amino acids and their compounds belong to a family of organic materials that have applications in NLO [8-11] as they contain a proton donor carboxyl acid (COO^-) group and the proton acceptor amino (NH_2) group in them. For example L-arginine and L-arginine phosphate, have shown second harmonic generation efficiency and are being applied in devices such as optical parametric amplifiers [12].

In the case of metal-organic coordination complexes, the organic legend is usually more dominant in the NLO effect. Since metal compounds have high transparency in the UV region (because of their closed d10 shell), there has been focus on the group (IIB) metals such as Zn, Cd, and Hg [13]. Due to these potential sites it was suggested to use zinc as dopant with L-PCCM crystal. In this paper, synthesis, bulk crystal growth and characterization of zinc doped L-proline cadmium chloride (Zn:LPCCM) have been discussed in detail.

2. Synthesis and growth

The starting material has been synthesized by taking 80% molecular weight of cadmium chloride and the 20% molecular weight of zinc chloride added with one molecular weight of L-proline in double distilled water at room temperature. The synthesized of Zn:LPCCM salt has been achieved by the following chemical reaction

$ZnCl_2$ (0.2mol) $+$ $CdCl_2$ (0.8mol).H_2O_+

$NHCH_2CH_2CH_2CHCOOH \rightarrow$

$$\frac{Cd(0.8mol)}{Zn(0.2mol)}NHCH2\ CH_2\ CH_2CHCOOH\ Cl_2\ H_2\ O$$

The 80% molecular weight of cadmium chloride was first dissolved in 100ml Millipore water of 18.2MΩcm resistivity. L-proline was added to the solution and later 20% of the $ZnCl_2$ was also added. The solution was stirred well by a magnetic stirrer. Then it was double times flittered with wattmann filter paper and poured into Petri dishes. The prepared solution was allowed to dry at room temperature and the salt was obtained by slow evaporation technique. The purity of the synthesized salt was further improved by successive recrystallization process. The seed obtained from the slow evaporation method has been used for the bulk growth. In a period of 50 to 55 days, the bulk crystal has formed with dimension 47×14×3.7 mm^3. The Fig. 1 shows the as grown crystal of Zn:LPCCM. It has been observed that crystals have good transparency, defect free and no inclusion. No microbes have been observed during the growth of Zn:LPCCM, probably chloride components which acted destructively over the growth of microbes [14].

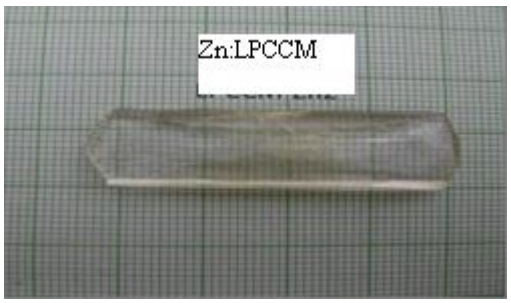

Fig. 1. As grown crystal of Zn:LPCCM.

3. Instrumentation

A suitable crystal was selected for single crystal XRD by using Xcalibur, Eos diffractometer. The crystal was kept at 293(2) K during data collection. To identify the reflection planes, powder X-ray diffraction pattern of the powdered sample was analysed using a Reich seifert diffractometer with CuKα (λ = 1.5418 A^0) radiation at 30 KV, 40 mA. The sample was scanned over the range of 10° to 50° at a scan rate of 2°/minute. The Fourier transform infrared spectroscopy was effectively used to identify the functional groups of the grown crystals. The FTIR spectrum of the sample was recorded using a Alpha bruker , alpha sample compartment RT-DLa TGS Znse with the maximum resolution of 2.00 cm^{-1} by the KBr pellet technique in the range 400–4000 cm^{-1}. The optical transmission spectrum of Zn:LPCCM crystal was recorded in the region 100–1000 nm using a VARIAN CARY 5000 spectrophotometer. Simultaneously thermogravimetric (TG) and differential thermal analyses (DTA) were carried out for Zn:LPCCM sample using a Seiko TG/DTA 6200 model thermal analyzer in nitrogen atmosphere. Powder sample of 15 mg was used for the analysis in the temperature range of 30–800°C with a heating rate of 20°C/minute. The NLO property was tested using a modified set-up of Kurtz and Perry and it was carried out using Q-switched mode locked Nd:YAG laser with output at 1064 nm. Microhardness measurements were made on as grown flat face grown crystal using Leitz-Weitzlar hardness tester fitted with a Vickers diamond indenter. The grown crystals were powdered and then made as a pellet for impedance spectroscopy studies using an impedance analyzer HT4284A precision LCR meter from 20 Hz to 1 MHz.

4. Results and discussion

4.1 Single crystal X-ray diffraction analysis

Single crystal X-ray diffraction analysis of Zn: LPCCM crystal has been carried out and the lattice parameter values are given in the Table 1.

Table 1. Lattice parameter values of the Zn:LPCCM crystal.

Crystal	a(Å)	b(Å)	c(Å)	V($Å^3$)	α = β = γ
Zn:LPCCM	10.0123(6)	13.5496(7)	7.2990(3)	990.18(15)	90°

From the result it has been found that Zn:LPCCM crystals belonged to orthorhombic system with space group of $P2_12_12_1$. The Zn:LPCCM cell parameters a,b, c and volume of unit cell, have been compared with L-PCCM crystal's cell parameters. The cell parameters of L-PCCM crystal are a= 9.952 Å, b=13.484 Å, c =7.255 Å and v=973.6 $Å^3$ [15]. The increase in cell parameter of Zn:LPCCM confirmed the incorporation of $ZnCl_2$, in L-PCCM crystal lattice.

4.2 Powder X-ray diffraction analysis

The crushed fine powder of Zn:LPCCM crystal has been subjected to powder X-ray diffraction analysis using a Reich seifert diffractometer with CuKα ($\lambda = 1.5418\ A^0$) radiation. The sample has been scanned over the range from 10° to 50° at a scan rate of 2°/minute and the recorded X-ray diffraction pattern of Zn:LPCCM has been indexed as shown in Fig. 2. The well defined Bragg's peak revealed the crystalline nature of the grown Zn:LPCCM crystal.

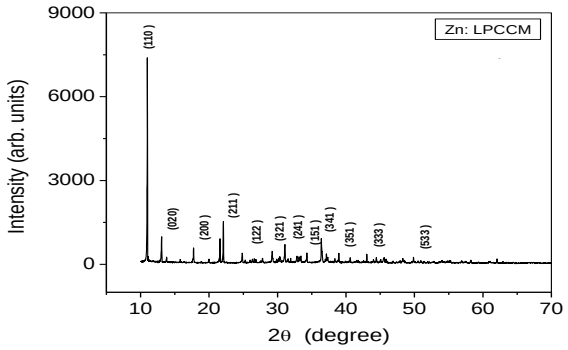

Fig. 2. Powder X-ray diffraction pattern of Zn:LPCCM crystal.

4.3 Fourier Transform infrared (FTIR) spectral studies

The Zn:LPCCM crystal's FTIR spectral analysis is shown in Fig. 3. In Zn:LPCCM spectrum, the peak at 3452 cm^{-1} has been assigned to the O-H stretching vibration of H_2O (O-H). The peaks at 3138 and 2742 cm^{-1} are the characteristics of $C_5H_9\ NO_2^+$. The lack of IR band at 1700 cm^{-1} clearly showed the existence of the COO^- ion in zwitterionic form [16]. The peak at 1591 cm^{-1} has been assigned to NH_2^+ in plane deformation. The peak at 1543 cm^{-1} has been assigned to NH_2^+ in plane deformation of L-proline cadmium chloride monohydrate. The characteristic of NH vibration has been observed at 1429 cm^{-1}.The other peaks at 1332 and 1282 cm^{-1} have been assigned to wagging of CH_2 group of the Zn:LPCCM. The rocking and wagging vibrations of COO^- have been observed at 483 and 633 cm^{-1} respectively. The linear frequencies of $ZnCl_2$ and $CdCl_2$ have occurred at 553 and 406 cm^{-1} respectively. The presence of all functional groups has been confirmed from FTIR spectrum [17]. The other observed wave numbers and their corresponding assignments have been presented in Table 2.

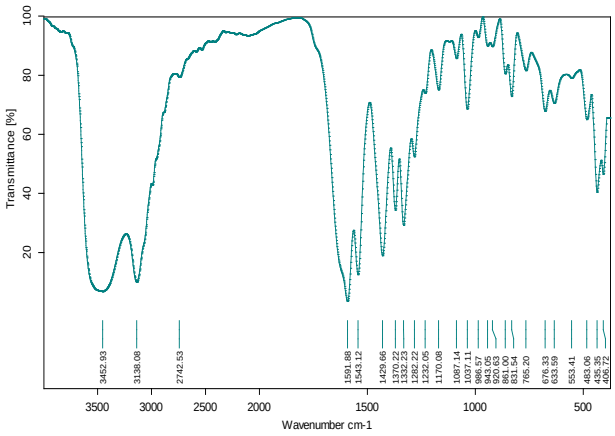

Fig. 3. FTIR spectrum of Zn:LPCCM crystal.

Table 2. Band assignment of FTIR spectra for Zn:LPCCM crystal.

Assignments	Zn:LPCCM crystal Wave number cm^{-1}
Stretching vibration of H_2O molecule	3452.53
N-H Stretching vibration	3138.08
N-H Stretching vibration	2742.53
NH_2^+ in plane deformation	1591.88
NH_2^+ in plane deformation	1543.12
COO^- Symmetric Stretching	1429.66
Wagging NH_2^+	1370.22
Wagging CH_2^+	1332.23
Wagging CH_2^+	1282.22
C-O Stretching	1232.05
Twisting NH_2^+	1170.08
NH_2^+ vibration	1087.14
C- N Stretching	1037.11
Rocking CH_2	986.57
Rocking CH_2	943.05
Rocking NH_2^+	920.63
Rocking CH_2	861.00
Rocking CH_2	831.54
In- plane deformation of COO^-	765.20
In- plane deformation of$CONH_2$	676.33
Wagging COO^-	633.59
Linear vibration of $ZnCl_2$	553.41
Rocking COO^-	483.06
Linear vibration of $CdCl_2$	406.72

4.4 Optical transmittance study

For better applications of NLO materials, wide optical transparency is an essential property. The optical transmittance spectrum of the grown Zn:LPCCM crystal has been recorded in the region 100-1000 nm, using a VARIAN CARY 5000 spectrophotometer. The recorded optical transmittance spectrum is shown in Fig. 4. The crystal has been found to be very transparent, about 80%, in the entire visible region. The transparency of the grown crystal agreed with the reported one [18]. The Zn:LPCCM crystal has the lower cut off wavelength at 209 nm in the UV region. Hence the Zn:LPCCM can be used as sensor material in the region from 800 to 209 nm and therefore it may also be used as UV sensors.

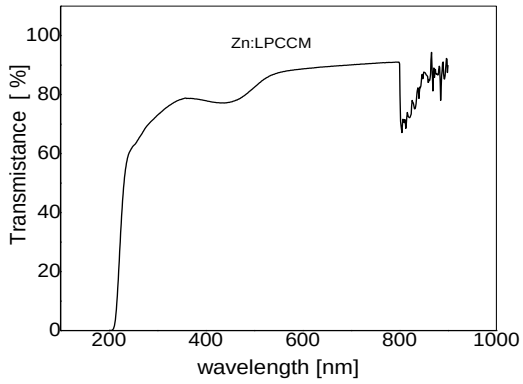

Fig. 4. Optical Transmission Spectrum of Zn:LPCCM crystal.

4.5 Thermal analysis

In order to study the thermal stability of the grown crystal, the thermo gravimetric (TG) and Differential thermal analysis (DTA) of Zn:LPCCM has been carried out using a Seiko TG/DTA 6200 model thermal analyzer in nitrogen atmosphere. Powder sample of 15 mg was used for the analysis in the temperature range of 30–800°C with a heating rate of 20°C/minute. The thermogram and differential thermogram are shown in Fig. 5. From the TG curve, it has been observed that there is no loss of weight upto 84°C. Above 84.1°C, H_2O which was in cadmium chloride started to decompose. Zinc doped L-proline cadmium chloride crystal posses thermal stability upto 207.0°C. At 207.1°C L-proline decomposed and it started to melt, it quit agreed with reported value 209°C [19]. At 350°C zinc chloride has started to melt and at 565.9°C cadmium chloride has started to melt. The residual components 15.2% in Zn:LPCCM crystal decomposed very slowly up to 800°C as shown in the DTA curve. Hence the grown Zn:LPCCM crystal has thermal stability upto 207.0°C.

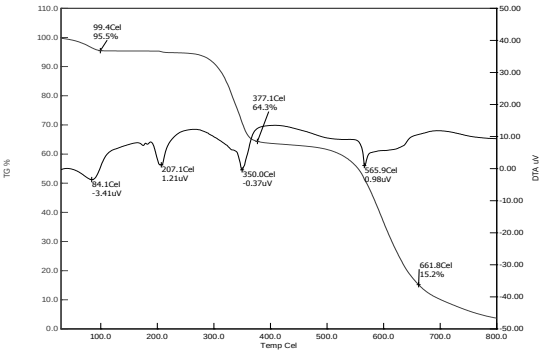

Fig. 5. TG/DTA Curves of Zn:LPCCM crystal.

4.6 Second harmonic generation efficiency test

The SHG analysis of Zn:LPCCM has been studied by Kurtz powder technique. The crystal was powdered and packed in a quartz capillary tube. An Nd:YAG laser beam at 1064 nm was made to fall on the powdered crystal. A green light was emitted from the powered crystal which confirmed that the grown Zn:LPCCM has SHG efficiency.

4.7 Microhardness test

The structure and molecular composition in crystals greatly influenced the mechanical properties. Microhardness measurements have been made on as grown flat face of Zn:LPCCM crystals using Leitz-Weitzlar hardness tester fitted with a Vickers diamond indenter. Hardness of the material is a measure of the resistance it offers to local deformation [20]. The Vicker's microhardness number, Hv has beeb calculated using the relation, $H_v = 1.8544\ (P/d^2)\ kg/mm^2$ [21] where P is the indenter load in gram and "d" is the diagonal length in mm of the impression. The variation of hardness H_v with load P ranging from 10 to 60 g on the flat surface of Zn:LPCCM crystal is shown in Fig. 6. This type of behavior wherein the hardness number increases with increase in applied load is called reverse indentation size effect [22]. From the higher hardness value of the grown crystal, it is inferred that greater stress is required to form dislocations and the crystals do not have any liquid inclusions.

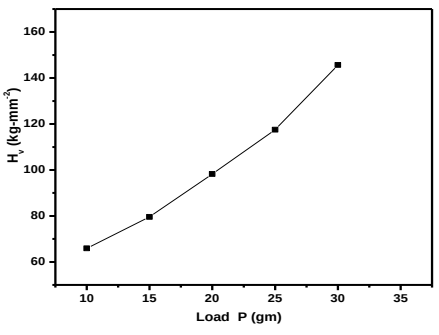

Fig. 6. Variation of hardness H_v with load P of Zn:LPCCM crystal.

4.8 Dark and photo currents studies

The photo conducting nature of the grown crystal has been estimated by using dark and photo currents studies. The field dependent of dark and photo currents of Zn:LPCCM crystals is shown in the Fig. 7. It has been observed that both dark current and photo current increase linearly with applied electric field. It also observed that the photo current is less than the dark current which implies that the grown Zn:LPCCM crystal has negative photo conductivity. The negative photoconductivity exhibited by a sample may be due to the reduction in the number of charge carriers in the presence of radiation [23]. The decrease in mobile charge carriers during negative photoconductivity can be explain by stockman model also, which is reported elsewhere [24].

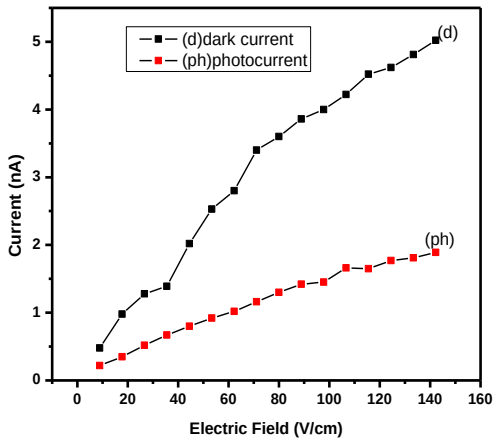

Fig. 7. Dark and Photo current graph of Zn:LPCCM crystal.

4.9 SEM-EDS analysis

The presence of Zinc as the doped specimen has been confirmed by EDS spectrum and the concentration of the incorporated zinc into the L-PCCM crystalline matrix can be clearly seen in Fig. 8. Analysis of the surface at different sites reveals that the incorporation of Zn is non- uniform over the whole crystal surface(SEM diagram is not shown).

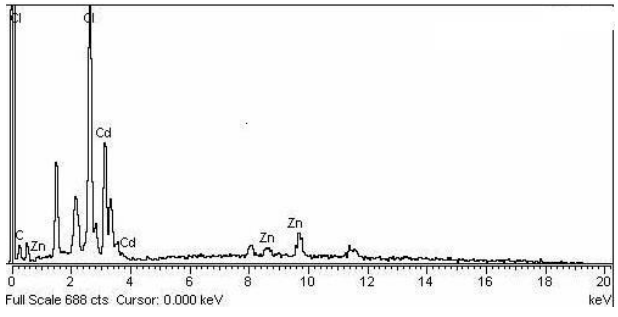

Fig. 8. Energy dispersive spectrum of Zn:LPCCM crystal.

4.10 Impedance spectroscopy

The complex impedance spectrum of the grown crystal is shown in Fig. 9. The graph has been plotted in the complex plane represented by the real part versus imaginary part (cole-cole plot) at several temperatures. Due to the high-frequency limitation of the used impedance analyzer, incomplete semicircles have been obtained at low temperatures. Some of the semi circles are incomplete, because the resistivity of the crystal is very large at low temperatures. The diameter of the arc and bulk resistance will be decreased with increasing temperature. The electrical conductivity is proportional to temperature. It indicates that the mobile ion has surface electrode effect at higher temperature.

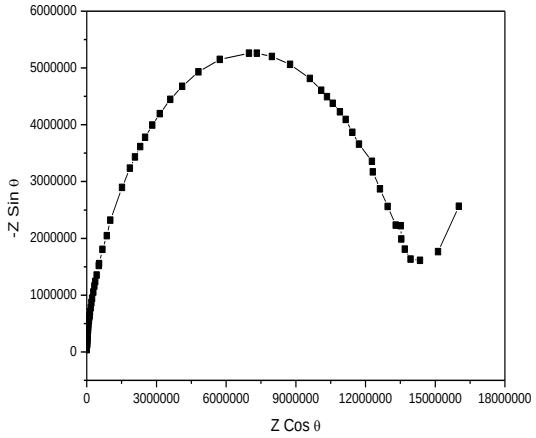

Fig. 9. Complex impedance spectrum of the Zn:LPCCM crystal.

5. Conclusion

The Zn:LPCCM crystal has been grown successfully in bulk size by adopting slow evaporation technique at room temperature. The grown crystal has been characterized by single crystal and Powder X-ray diffraction method. The functional groups have been confirmed by FTIR spectrum. The grown crystal has been found to be transparent from 209 to 1000 nm and thus confirming in wider optical transmission range. Thermal stability of the crystal has been found to be 207˚C. SHG studies confirmed the Nonlinear optical property of the grown Zn:LPCCM crystal. Microhardness measurement shows the grown crystal had reverse indentation size effect. Dark and Photo currents Studies implied that the grown Zn:LPCCM crystal had negative photo conductivity. The doping of Zinc has been confirmed by EDS spectrum. Impedance spectrum indicates that the mobile ion of Zn:LPCCM possess surface electrode effect at higher temperature.

Acknowledgement

The authors acknowledge Dr. R. Jayavel, Director, Center for Nanoscience and Technology, Anna University, Chennai-25 and Dr. S. M. Ravikumar, Govt. Arts College, Tiruvannamalai, for their continuous encouragement in pursuing the above research. Authors also acknowledge Dr. Binoy Krishna Saha, Assistant Professor of Chemistry, Pondicherry University for providing single crystal XRD facility, B. S. Abdur Rehman University for NLO and TGA/DTA studies, VIT University for powder XRD studies.

References

[1] G. Madurambal, M. Mariyappan, S. Monojumdar, J. Therm. Anal. Calorim. **100**, 853 (2010).
[2] D. S. Chemla, J. Zyss, Eds. Nonlinear Optical Properties of Organic Molecules and Crystals; Academic Press: New York, (1987).
[3] P. N. Prasad, D. J. Williams, Introduction to Nonlinear Optical Effects in Molecules and Polymers; Wiley-Interscience: New York, (1991).
[4] R. Rajasekaran, P. M. Ushashree, P. Jayavel, J. Ramasamy, J. Cryst. Growth **229**, 563 (2001).
[5] K. J. Arun, S. Jayalakshmi , J. Minerals & Materials Characterization & Engineering **8**, 635 (2009).
[6] G. Madurambal, M. Mariyappan , S. Monojumdar , J. Therm. Anal. Calorim. **100**, 763 (2010).
[7] S. Gopinath, S. Barathan, R Rajasekaran. J. Therm. Anal. Calorim. DOI 10.1007/s10973-011-1775-3.
[8] D Xu., M Jiang, Z Tan, Acta Chem. Sinica, **41**, 570 (1983).
[9] M. Kitazawa, R. Higuchi, M. Takahashi, Appl. Phys. Lett. **64**, 2477 (1994).
[10] L. Misoguti, A. T. Varela, F. D. Nunes, V. S. Bagnato, F. E. A. Melo Mendes J Filho, C. Zilio, Opt. Mater. **6**, 147 (1996).
[11] W. S. Wang, M. D. Aggarwal, J. Choi, T. Gebre, A. D. Shields, B. G. PennFrazier, J. Cryst. Growth, **578**, 198 (1999).
[12] S. B Monaco, L. E. Davis, S. P. Velsko, F. T. Wang, D. Eimerl, A Zalkin, J. Cryst. Growth **85**, 252 (1987).
[13] S. Dhanuskodi, K. Vasantha, P. A. Angeli Mary, Spectrochim. Acta Part A **66**, 637 (2007).
[14] A. Kandasamy, R. Siddeswaran, P. Murugakoothan, P. Sureshkumar, R. Mohan, Synthesis, Crystal Growth & Design **7**(2), 183(2007).
[15] Y. Yukawa, Y. Inomata, T. Takeuchi, Bill. chem. soc. Jpn. **56**, 2125 (1983).
[16] H. Ratajczak, J. Baryck, A. Pietraszko, S. Debrus, M. May, J. Venturini. Cryst, J. Mol. Struct., **526**, 269 (2000).
[17] K. Nakamoto, Infrared and Raman spectra of Inorganic and Coordination Compounds, Wiley, New York, (1978).
[18] S. K. Mohd. Shakir, K. K. Kushwaha, R. C. Maurya Bhatt, Rashmi, M. A. Wahab, G. Bhagavannarayana Mater. Chem. Phy., **120**, 566 (2010).
[19] Thomas Joseph Prakash, S. Kumararaman, J, Mater. lett. **62**, 4097 (2008).
[20] Mary Linet, S. Jerome Das, Physica B, **405**, 3955 (2010).
[21] B. W. Mott, "Microindentation Hardness Testing", Butterworths, London, (1956).
[22] K. Sangwal, M. Hordyjewicz, B. Surowska, J. Optoelectron. Adv. Mater. **4**, 875 (2002).
[23] S. Abrham Rajasekar, K. Thamizharasan, J. G. M. Jesudurai, D. Prem Anand, P. Sagayaraj, Mater. Chemistry. Physics **84**, 157 (2004).
[24] V. N. Joshi, Photoconductivity, Marcel Dekker, Newyork, 1990.

*Corresponding author: vetrivelsivaraman@yahoo.com